

# Research on Three-phase Grid-connected Photovoltaic Power Generation System

<sup>1</sup>Ch. Hao, <sup>1</sup>S. Yang, <sup>1</sup>X. Wang, <sup>1</sup>N. Rui And <sup>2</sup>Alexey Shumsky

**Abstract**—With the development of world economic and shortage of energy, Research on solar photovoltaic power generation system is of great theoretical and practical significance in alleviating energy and environmental problems, improving the energy consumption structure and the performance of distributed generation systems. Under this background, this paper focus on the three-phase grid-connected photovoltaic power generation system, in the terms of hardware system design, control algorithm and system simulation. In this paper, module of three-phase grid-connected photovoltaic power generation system is established. A variable step-size maximum power point tracking control strategy is proposed. And a control algorithm named double d-q axis phase-locked loop is proposed. Simulation is verified in the form of hardware.

**Keywords**—photovoltaic; MPPT; SVPWM; phase-locked loop; output power

## I. INTRODUCTION

Photovoltaic is a green and renewable energy which has the advantages of no noise and no limit of terrain. However, the disadvantage of low conversion efficiency and high price is also obvious. So how to use the photovoltaic energy efficiently on the basis of the present condition is an important direction of the research photovoltaic. When one photovoltaic system is at a changing external condition, the maximum power point tracking (MPPT) control become the key to improve the efficiency of photovoltaic system.

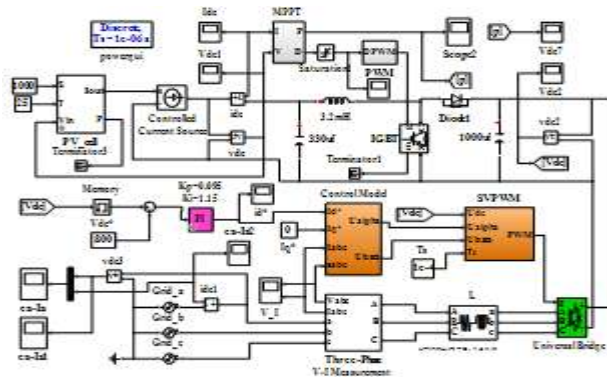


Fig. 1. Three - phase photovoltaic grid - connected system Simulation model.

achieve phase-locked loop. The traditional phase-locked loop can not accurately track the phase when the grid voltage is unbalanced, so we propose a control algorithm named double d-q axis phase-locked loop to eliminate AC component in feedback and make sure the phase is tracked accurately.

## II. THE ESTABLISHMENT OF SYSTEM SIMULATION MODEL

The main model is shown in the Fig.1. This model uses Boost circuit as the DC-DC circuit. There are photovoltaic cell model “PV cell”, maximum power point tracking module “MPPT”, space vector module “SVPWM”, “control module” including phase locked loop module “3 phase PLL”, Three-Phase voltage and current measurement module “Three-Phase V-I Measurement”, three-phase full-bridge inverter “Universal Bridge”.

The maximum power point tracking module is shown in Fig.2. As is shown in Fig.1 and Fig.2, the input of maximum power point tracking model, “I” and “V”, are the output current and voltage of the PV cell. The output of maximum power point model, “D”, is duty cycle applied to IGBT. In this MPPT, we give a perturbation to the system, and if this perturbation cause a rise of output power, we will continue this perturbation, if not, we will give a reverse perturbation.

$$R'_L = R_L(1-D)^2 \quad (1)$$

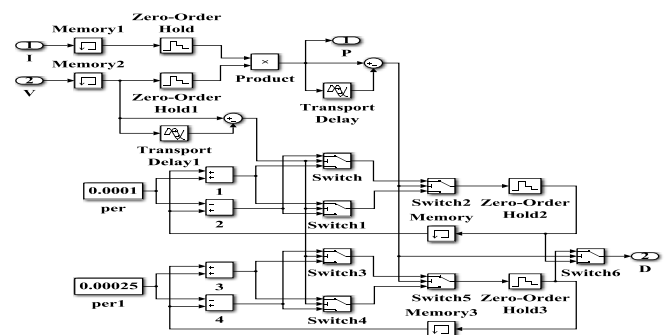


Fig. 2. Maximum power point control module.

<sup>1</sup>China University of Mining and Technology, Xuzhou, 221116 China

<sup>2</sup>Russian Academy of Sciences, Far Eastern Branch, Vladivostok, Russia

The relationship of equivalent impedance  $R'_L$ , load resistance  $R_L$  and duty cycle  $D$  is shown in equation[1] (1). Change the equivalent impedance by control the duty cycle to

match the output resistance of PV cell. The input voltage subtracts its value last moment which is delayed  $10^{-4}$  s through a Transport Delay. Switch, Switch1, Switch3 and Switch4 choose the above one if the value of the input voltage subtracts its value last moment greater than 0, otherwise it chooses the below one. The input current and voltage is multiplied through Product to get the value of power. The value of power is delayed  $10^{-4}$  s through a Transport Delay, and it is compared with the value without delay. And if the value of the difference between value of power and the value delayed is greater than 0.03, Switch6 will choose 0.00025 as step, otherwise it chooses 0.0001 as step.

The control module is shown in Fig.2. As is shown in Fig.1 and Fig.3, the input of this module are: three - phase grid voltage  $e_{abc}$ , three - phase grid current  $i_{abc}$ , reference current signal  $I_d^*$  and reference signal  $I_q^*$ . The difference between DC bus voltage  $V_{dc}$  and reference signal  $V_{dc}^*$  come through a PI controller and get the value of  $I_d^*$ . And the reference signal  $I_q^*$  is usually set 0 so that the power factor is 1. In this module, we want the  $u_\alpha$  and  $u_\beta$  which is phase tracked for the module “SVPWM”, so we need to do work shown in Fig.3.

First, we need the get the grid voltage phase locked with module “3 phase PLL”. For low-voltage distribution network, due to the imbalance of electricity load, three-phase voltage asymmetry is in a high proportion, and power grid failure will lead to three-phase voltage asymmetry too. So what is shown in the module is in the situation of unbalanced grid voltage. As is shown in Fig.3 and Fig.4. When three-phase voltage is symmetrical,  $e_{abc}$  is transformed to  $u_d$  and  $u_q$  by Clark transformation and Park transformation to the following equation[2] (2):

$$\begin{bmatrix} u_d \\ u_q \end{bmatrix} = \begin{bmatrix} U_{m1} \cos(\omega t - \hat{\theta}) \\ U_{m1} \sin(\omega t - \hat{\theta}) \end{bmatrix} \quad (2)$$

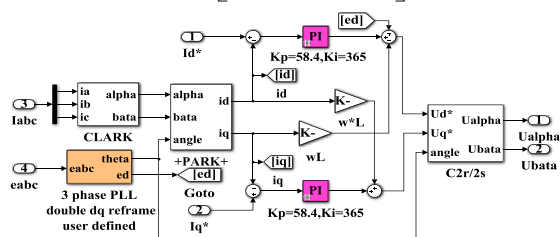


Fig. 3. Control module.

When phase-locked loop is locked,  $\omega t - \hat{\theta} = 0$ ,  $u_q = 0$ . However, when three-phase grid voltage is asymmetric,  $u_a$ ,

Copyright © Authors

$u_b, u_c$  can be written in the form shown in the following equation[2]:

$$\begin{bmatrix} u_a \\ u_b \\ u_c \end{bmatrix} = \begin{bmatrix} U_{m1} \cos(\omega t) + U_{m2} \cos(-\omega t + \psi^{-1}) + U_{m0} \cos(\omega t + \psi^0) \\ U_{m1} \cos(\omega t - \frac{2}{3}\pi) + U_{m2} \cos(-\omega t - \frac{2}{3}\pi + \psi^{-1}) + U_{m0} \cos(\omega t + \psi^0) \\ U_{m1} \cos(\omega t + \frac{2}{3}\pi) + U_{m2} \cos(-\omega t + \frac{2}{3}\pi + \psi^{-1}) + U_{m0} \cos(\omega t + \psi^0) \end{bmatrix} \quad (3)$$

It can be transformed by Clark transformation and Park transformation to equation[2] (4):

$$\begin{bmatrix} u_d \\ u_q \end{bmatrix} = \begin{bmatrix} U_{m1} \cos(\omega t - \hat{\theta}) + U_{m2} \cos(-\omega t - \hat{\theta} + \psi^{-1}) \\ U_{m1} \sin(\omega t - \hat{\theta}) + U_{m2} \sin(-\omega t - \hat{\theta} + \psi^{-1}) \end{bmatrix} \quad (4)$$

We can see that there is an AC component in  $u_q$ . This component will result in an error in phase-locked loop. As a result, it is necessary to eliminate AC component in  $u_q$ . As is shown in Fig.4, the output of Clark transformation  $u_\alpha$  and  $u_\beta$  is transformed by Park transformation to equation [3] (5):

$$\begin{bmatrix} u_{d+} \\ u_{q+} \end{bmatrix} = \begin{bmatrix} U_{m1} \cos(\omega t - \hat{\theta}) + U_{m2} \cos(-\omega t - \hat{\theta} + \psi^{-1}) \\ U_{m1} \sin(\omega t - \hat{\theta}) + U_{m2} \sin(-\omega t - \hat{\theta} + \psi^{-1}) \end{bmatrix} \quad (5)$$

In formula(5),

$$\begin{aligned}
u_{q+} &= U_{m1} \sin(\omega t - \hat{\theta}) + U_{m2} \sin(-\omega t - \hat{\theta} + \psi^{-1}) \\
&= U_{m1} \sin(\omega t - \hat{\theta}) + U_{m2} \sin(-\omega t - \hat{\theta}) \cos \psi^{-1} + U_{m2} \cos(-\omega t - \hat{\theta}) \sin \psi^{-1}
\end{aligned} \tag{6}$$

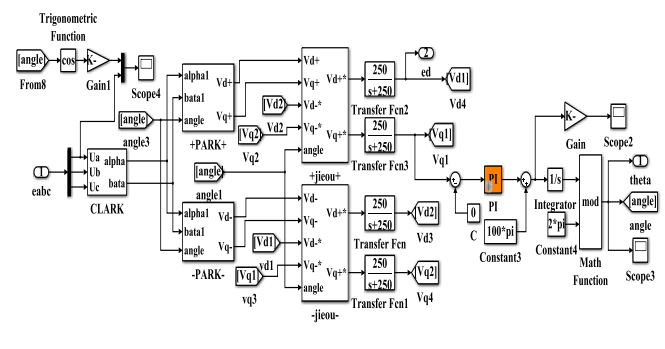


Fig. 4. Double d-q axis phase-locked loop module.

subset  $A$  of  $I$  and non-empty subset  $O$  of  $T$ , the two And the output of Clark transformation  $u_\alpha$  and  $u_\beta$  is transformed by a negative Park transformation to equation[4] (7):

$$\begin{bmatrix} u_{d-} \\ u_{q-} \end{bmatrix} = \begin{bmatrix} U_{m1} \cos(\omega t + \hat{\theta}) + U_{m2} \cos(-\omega t + \hat{\theta} + \psi^{-1}) \\ U_{m1} \sin(\omega t + \hat{\theta}) + U_{m2} \sin(-\omega t + \hat{\theta} + \psi^{-1}) \end{bmatrix} \quad (7)$$

by a negative Park transformation according to the following equation[4]:

$$\begin{bmatrix} u_{d-} \\ u_{q-} \end{bmatrix} = \begin{bmatrix} \cos \hat{\theta} & -\sin \hat{\theta} \\ \sin \hat{\theta} & \cos \hat{\theta} \end{bmatrix} \begin{bmatrix} u_{\alpha} \\ u_{\beta} \end{bmatrix} \quad (8)$$

Assume that

$$\begin{bmatrix} u_{d-} \\ u_{q-} \end{bmatrix} = \begin{bmatrix} \bar{u}_{d-} \\ \bar{u}_{q-} \end{bmatrix} + \begin{bmatrix} \dot{\bar{u}}_{d-} \\ \dot{\bar{u}}_{q-} \end{bmatrix}, \quad \begin{bmatrix} \bar{u}_{d-} \\ \bar{u}_{q-} \end{bmatrix} = \begin{bmatrix} U_{m1} \cos(\omega t + \hat{\theta}) \\ U_{m1} \sin(\omega t + \hat{\theta}) \end{bmatrix}, \quad (9)$$

$$\begin{bmatrix} \dot{\bar{u}}_{d-} \\ \dot{\bar{u}}_{q-} \end{bmatrix} = \begin{bmatrix} U_{m2} \cos(-\omega t + \hat{\theta} + \psi^{-1}) \\ U_{m2} \sin(-\omega t + \hat{\theta} + \psi^{-1}) \end{bmatrix}$$

When  $\omega t - \hat{\theta} = 0$ , formula(5) can be transformed to:

$$u_{q+} = 0 + \dot{\bar{u}}_{d-} \sin(-2\hat{\theta}) + \dot{\bar{u}}_{q-} \cos(-2\hat{\theta}) \quad (10)$$

We can get  $\begin{bmatrix} u_d \\ u_q \end{bmatrix}$  and  $\begin{bmatrix} u_{d-} \\ u_{q-} \end{bmatrix}$  decoupled. After this, when

$$\omega t - \hat{\theta} = 0, u_{q+} = 0.$$

As a result, phase angle can be accurately locked through three-phase voltage phase locked loop mentioned in this paper.

Inverter topology is shown in Fig.5.

In order to transform  $U_a, U_b$  and  $U_c$  to  $U_{\alpha}$  and  $U_{\beta}$ , it is necessary to do works shown in Fig.3.

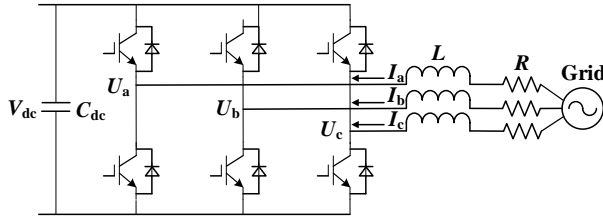


Fig. 5. Inverter topology.

As is shown in Fig.5, we can get the following equation[2]:

$$\begin{aligned} u_a &= Ri_a + L \frac{di_a}{dt} + e_a \\ u_b &= Ri_b + L \frac{di_b}{dt} + e_b \\ u_c &= Ri_c + L \frac{di_c}{dt} + e_c \end{aligned} \quad (11)$$

After Clark transformation and Parker transformation, formula(11) is transformed to equation[4] (12):

$$\begin{bmatrix} L \frac{di_d}{dt} \\ L \frac{di_q}{dt} \end{bmatrix} = \begin{bmatrix} -R & \omega L \\ \omega L & -R \end{bmatrix} \begin{bmatrix} i_d \\ i_q \end{bmatrix} + \begin{bmatrix} 1 & 0 \\ 0 & 1 \end{bmatrix} \begin{bmatrix} u_d \\ u_q \end{bmatrix} - \begin{bmatrix} 1 & 0 \\ 0 & 1 \end{bmatrix} \begin{bmatrix} e_d \\ e_q \end{bmatrix} \quad (12)$$

When  $\omega t - \hat{\theta} = 0$ ,  $e_d = E_s$ ,  $e_q = 0$ . Write formula(12) in

$$\begin{aligned} L \frac{di_d}{dt} + Ri_d &= u_d - E_s + \omega Li_q \\ L \frac{di_q}{dt} + Ri_q &= u_q - \omega Li_d \end{aligned} \quad (13)$$

Assume that

$$\begin{aligned} u'_d &= L \frac{di_d}{dt} + Ri_d, \quad u'_d = K_p(i_d^* - i_d) + K_i \int (i_d^* - i_d) dt \\ u'_q &= L \frac{di_q}{dt} + Ri_q, \quad u'_q = K_p(i_q^* - i_q) + K_i \int (i_q^* - i_q) dt \end{aligned} \quad (14)$$

And we can get that

$$\begin{aligned} u_d^* &= E_s - \omega Li_q + u'_d \\ u_q^* &= \omega Li_d + u'_q \end{aligned} \quad (15)$$

In formula (15),  $E_s$  is grid voltage [ed], which is got in 3 phase PLL module. And then, after an Anti-Park transform,  $u_d^*$  and  $u_q^*$  is transformed to  $U_{alpha}$  and  $U_{bata}$ . So we get  $u_a, u_b, u_c$  Clark transformed through decoupling.

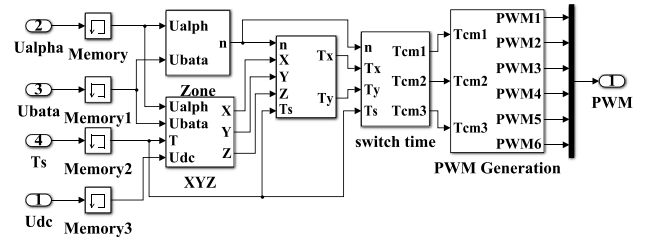


Fig. 6. SVPWM module.

As is shown in Fig.1 and Fig.6, inputs of "SVPWM" module are the output of DC-DC circuit " $V_{dc}$ " and output of "Control Module"  $U_{alpha}$  and  $U_{bata}$ . There are four modules with four different functions in "SVPWM" module.

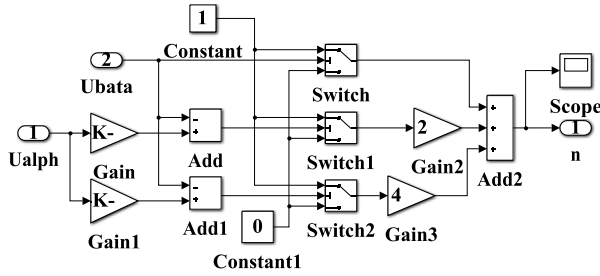


Fig. 7. Sector judgment module "Zone".

First is the sector judgment module "Zone" shown in Fig.8., there are eight states, and they can be shown in the form of eight space vectors as shown in Fig.7. Which sector should we choose depends on the relationship of  $U_\beta$ ,  $\sqrt{3}U_\alpha - U_\beta$ ,  $-\sqrt{3}U_\alpha - U_\beta$  and 0. Assume that  $A = U_\beta$ ,  $B = \sqrt{3}U_\alpha - U_\beta$ ,  $C = -\sqrt{3}U_\alpha - U_\beta$ ,  $P = \text{sgn}(A) + 2\text{sgn}(B) + 4\text{sgn}(C)$ .

Relationship of sector and value of P is shown in Table 1.

Table 1. Relationship Of Sector And Value Of P

Value of P	3	1	5	4	6	2
Sector	I	II	III	IV	V	VI

Second is action time calculating of basic vector. There are two modules, "XYZ" and "Choose" shown in Fig.9 and Fig.10 to achieve this function.

Here we take sector I as an example. We can figure that equation[5] (16):

$$\begin{cases} u_\alpha = \frac{T_1}{T_{PWM}}|U_1| + \frac{T_2}{T_{PWM}}|U_2|\cos\frac{\pi}{3} \\ u_\beta = \frac{T_2}{T_{PWM}}|U_2|\sin\frac{\pi}{3} \end{cases} \quad (16)$$

And from formula(16) we can get that equation[18] (17):

$$\begin{cases} T_1 = \left( \frac{3}{2}u_\alpha - \frac{\sqrt{3}}{2}u_\beta \right) \frac{T_{PWM}}{U_{dc}} \\ T_2 = \frac{\sqrt{3}u_\beta T_{PWM}}{U_{dc}} \end{cases} \quad (17)$$

Similarly, we can get action time of vector in other sectors. Assume that equation[5] (18):

$$\begin{cases} X = \frac{\sqrt{3}T_{PWM}u_\beta}{U_{dc}} \\ Y = \frac{\sqrt{3}T_{PWM}}{U_{dc}} \left( \frac{\sqrt{3}}{2}u_\alpha + u_\beta \right) \\ Z = \frac{\sqrt{3}T_{PWM}}{U_{dc}} \left( -\frac{\sqrt{3}}{2}u_\alpha + u_\beta \right) \end{cases} \quad (18)$$

And we can get action time shown in Table 2 of  $T_1, T_2$  in each sector.

Table 2. Action Time in Each Sector

N	I	II	III	IV	V	VI
$T_1$	Z	Y	-Z	-X	X	-Y
$T_2$	Y	-X	X	Z	-Y	-Z

If  $T_1 + T_2 > T_{PWM}$ ,  $T_1$  and  $T_2$  must be processed as equation[6] (19).

$$\begin{cases} T_1 = \frac{T_1}{T_1 + T_2} T_{PWM} \\ T_2 = \frac{T_2}{T_1 + T_2} T_{PWM} \end{cases} \quad (19)$$

Achievement of getting "XYZ" and processing  $T_1, T_2$  is shown in Fig.8 and Fig.9.

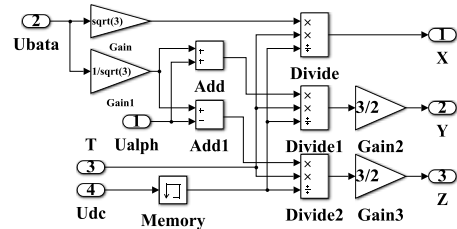


Fig. 8. "XYZ" module.

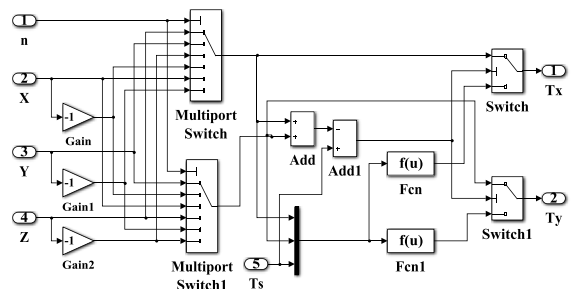


Fig. 9. "Choose" module.

The third part is “switch time” module. It’s function is determining vector switching time of each sector. Define that equation[6] (20):

$$\begin{cases} T_{cm1} = \frac{T_S - T_1 - T_2}{4} \\ T_{cm2} = \frac{T_S - T_1 - T_2}{4} + \frac{T_1}{2} \\ T_{cm3} = \frac{T_S - T_1 - T_2}{4} + \frac{T_1}{2} + \frac{T_2}{2} \end{cases} \quad (20)$$

and assume that equation[6] (21):

$$\begin{cases} T_a = \frac{T_S - T_x - T_y}{4} \\ T_b = T_a + \frac{T_x}{2} \\ T_c = T_b + \frac{T_y}{2} \end{cases} \quad (21)$$

In order to reduce switching losses, we must choose zero vector 000 and 111 reasonably to change status of only one MOSFET at a time. Take sector I as an example, status of MOSFET in inverter is  $U_0$  (000),  $U_1$  (100),  $U_2$  (110),  $U_7$  (111),  $U_2$  (110),  $U_1$  (100),  $U_0$  (000). Similarly, we can get the switching time of each sector as is shown in Table 3.

Table 3. Switching time of each sector

Sect or	I	II	III	IV	V	VI
$T_{cm1}$	$T_a$	$T_b$	$T_c$	$T_c$	$T_b$	$T_a$
$T_{cm2}$	$T_b$	$T_a$	$T_a$	$T_b$	$T_c$	$T_c$
$T_{cm3}$	$T_c$	$T_c$	$T_b$	$T_a$	$T_a$	$T_b$

The choice to switching time in Simulink is shown in Fig.10.

The last part is getting the PWM wave. As is shown in Fig.11, when the value of triangular carrier is bigger than  $T_{cm1}$ , output of “Relay” is 1, otherwise, the output is 0. So we get “PWM1” and we can get “PWM2” negating “PWM1”. Similarly, we can get control signal of other MOSFET.

Simulation shows that double d-q axis phase-locked loop can track the phase accurately. Three-phase voltage and current waveform in simulation is shown in Fig.12.

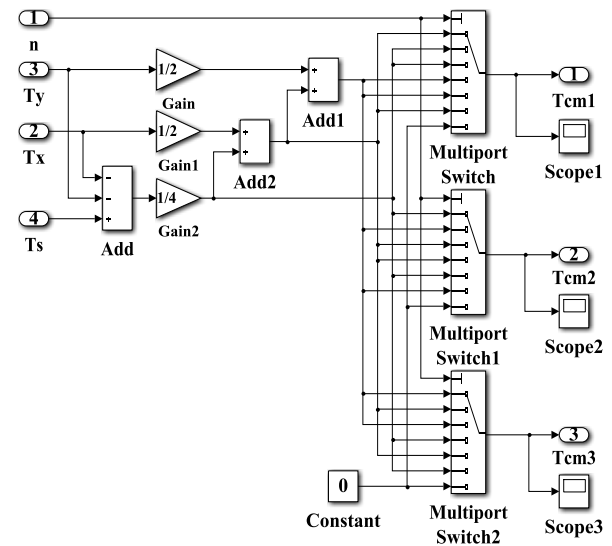


Fig. 10. Choice to switching time in Simulink.

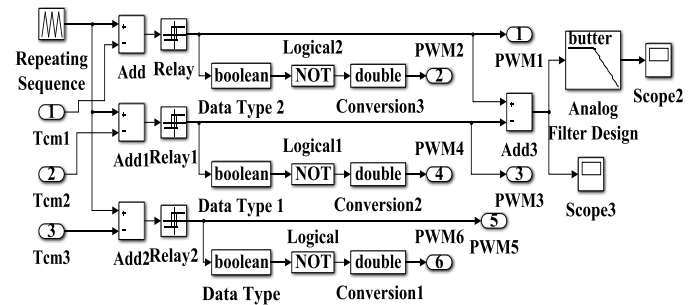


Fig. 11. Module to get PWM wave.

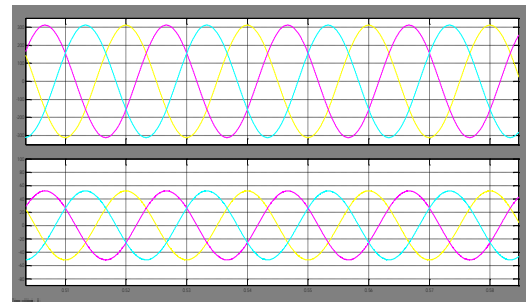


Fig. 12. Three-phase voltage and current waveform.

### III. EXPERIMENTAL VERIFICATION AND ANALYSIS

System physical photo is shown in Fig.13. The inductance parameter is 6mH, capacitance parameter is 100  $\mu F$  and the load is 100  $\Omega$ .



Fig. 13. System physical photo.

Fig.16 shows the light intensity is  $1000 W/m^2$  and temperature is  $25^\circ C$ , MPPT is variable step-size maximum power point tracking control strategy, waveform of PV cell from start to steady state in Simulation. Fig.16 shows the output power waveform in practical application. Fig.17 shows that sudden reduction happens in light intensity, waveform of the response process of PV cell.

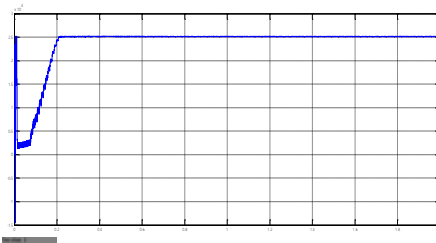


Fig. 14. Output power waveform of PV cell in Simulink.

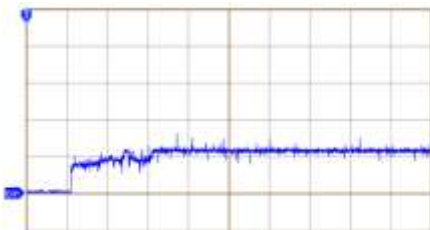


Fig.15. Output power waveform in practical application.

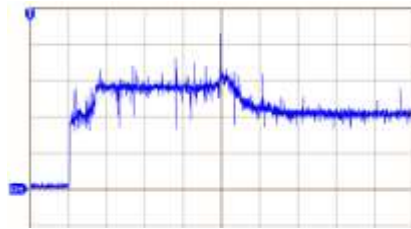


Fig. 16. Output power waveform when sudden reduction happens in light intensity.



Fig. 17. Experimental platform of inverter unit and AC source.

As is shown in Fig.15, 0~0.1s is the maximum power point searching process. At this time, the system will choose a larger step-size to rapidly increase the duty cycle. When a small change in the external environment, small steps can reduce system fluctuations. In Fig.16, during the steady state, a sudden reduction happens, and the system respond within 0.01s. At this time the external environment changes greatly, maybe cloud or planes, the system uses a larger step-size to change the duty cycle quickly to bring the system to a new steady state. Experimental results show that variable step-size maximum power point tracking control strategy can respond quickly and has good stability.

Experimental platform of inverter unit can be seen in Fig.17. DC bus voltage is 110V. AC load resistance in 58  $\Omega$ . Output voltage and current waveform of inverter circuit is shown in Fig.18. The ratio of each measuring value is on the longitudinal axis. Voltage is 40V per cell and current is 3.3A per cell. When system runs steadily, peak voltage reaches to 155V, effective value is 110V.

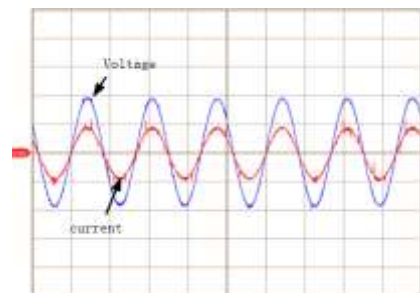


Fig. 18. Voltage and current waveform of Phase A when running steadily.

#### IV. CONCLUSION

The following conclusions can be drawn from the above research:

Based on the analysis of the mathematical model of photovoltaic cells and according to the actual use of parameters on the photovoltaic panel, a variable step-size maximum power point tracking control strategy is proposed. This control method makes the system can respond quickly and also has good stability.

Based on Simulation built in this paper and comparison of traditional phase-locked loop algorithm and double d-q axis phase-locked loop algorithm, the AC component in  $u_q$  happens in traditional phase-locked loop is eliminated. As a result, we can track phase accurately with the algorithm proposed in this paper.

Build hardware experimental platform and use DSP28335 programming, the experimental results show the correctness of the above conclusions.

#### ACKNOWLEDGMENT

This work was supported from the Xuzhou City Science and Technology Project-Science and Technology Cooperation under Grant KC16HG233.

#### REFERENCES

- [1] Liu F, Duan S, Liu F, et al. A variable step size INC MPPT method for PV systems. *IEEE Transactions on industrial electronics*, 2008, 55(7): 2622-2628.
- [2] Ruan Yi, Chen Boshi, et al. Control system of electric drives-motion control systems. China Machine Press.2009.8
- [3] Qiu Guanyuan, Luo Xianjue, et al. Electric circuit. Higher Educaiton Press. 2009.8.
- [4] Xin Yechun, Li Guoqing, et al. Study of three-phase voltage phase locked loop based on double dq transformation reference frame. *Power System Protection and Control*. 2014.5
- [5] Beig A R, Narayanan G, Ranganathan V T. Modified SVPWM Algorithm for Three Level VSI With Synchronized and Symmetrical Waveforms. *IEEE Transactions on Industrial Electronics*, 2007, 54(1):486-494.
- [6] Rajkumar M V, Manoharan P S. FPGA based multilevel cascaded inverters with SVPWM algorithm for photovoltaic system. *Solar Energy*, 2013, 87(1):229-245.